# The Influence of Underroof Systems on the Hygrothermal Behavior of Sloped Insulated Roofs

**A. Janssens** **H. Hens** **A. Silberstein** **J. Boulant**

## ABSTRACT

*In the light of discussions concerning the overall hygrothermal behavior of sloped roofs, experimental results obtained in a calibrated hot and cold box are discussed. The behavior of three sloped roofs, constructed as is common in France but with different underroof systems in terms of water vapor permeability and capillarity, has been simultaneously monitored. In this paper, measurements are presented and results interpreted. The test roof behavior shows that the use of an underroof system with good capillary properties and high vapor permeability, adapted in a "sandwich" section, is a good way to prevent moisture problems and excessive heat loss in sloped roofs insulated at rafter level.*

## INTRODUCTION

The need to make loft spaces part of the inhabited building created the necessity to increase the thermal resistance of sloped roof constructions to meet comfort and energy conservation demands. A practical way to obtain improved thermal performance is to install insulation between the rafters. Attaching a rain and wind barrier on the outside of the insulation layer (tiles/slates/underroof) and a nice finish on the inside could provide a practical and, at first sight, well-performing envelope. However, moisture and frost damage or problems with heating the lofts frequently occur. The traditional answer to prevent moisture problems, namely, to vent under the tiles and underroof, does not totally prevent damage. Previous research has shown that lack of airtightness is the main cause of the poor hygrothermal performance of sloped roofs insulated at rafter level (Hens et al. 1983; Hens 1992).

This paper tries to answer some additional questions related to sloped roof behavior. How sensitive to airtightness are energy losses and condensation problems in sloped roofs? What is the influence of underroof properties on these phenomena? These questions have been clarified by measuring temperatures, heat flows, and moisture migration in three test roofs under load of a temperature, partial water vapor, and air pressure difference, with a lengthy hot and cold box experiment.

## EXPERIMENTAL PROGRAM

### Test Roofs

The roof is divided into three sections, each constructed as an element (lxw = 2.14 m x 0.78 m) of a wood-frame roof insulated between the rafters: roof slope from horizontal, 60°; section of rafters, 45 mm x 120 mm; distance between centerlines, 367 mm. The sections are separated from each other by a double rafter with a vapor-tight bituminous layer inbetween. The three sections are referred to as Field 1, Field 2, and Field 3. The different parts of the roof section are conceived to be detachable in order to be able to follow their weekly change of weight.

#### Field 1 (to the outside) (Figure 1)

- Gypsum board: thickness $d$ = 12.5 mm, vapor permeability $\delta = 2.3*10^{-11}$ s; edges are closed with silicones; the board is attached to the rafters by means of a metal U-profile frame.
- Insulation of glasswool blankets: $d$ = 140 mm, density $\rho$ = 12.7 kg/m$^3$; the kraftpaper (d = 0.2 mm, $\delta = 7.9*10^{-15}$ s) on the warm side of the insulation is placed without special care for air- or vaportightness; half of the insulation can be taken out for weighing.
- Frame with underroof: hygrodiode membrane (capillary vapor retarder), d = 0.4 mm, $\delta = 4.0*10^{-14}$ s; the membrane is assembled in two parts with a horizontal overlap (= 100 mm) situated 1 m from the bottom edge and fixed on a wooden frame (2.10 m x 0.78 m); this frame is attached on the underlying rafters by means of bolts and nuts, in such a way that the junction is as air and vapor tight as possible; additional air supplies to ventilate the airspace (10 - 30 mm) between insulation and underroof are NOT installed.
- Six tile laths, 22 mm x 36 mm, dismountable.
- Twenty-four tiles (440 mm x 260 mm), double lock type; $\rho$ = 2020 kg/m$^3$, capillary moisture content $w_c$ = 205 kg/m$^3$.

#### Field 2

- The same as Field 1, except that another (vapor open) underroof is fixed in the wooden frame: a spun-bonded

**Arnold Janssens** and **Hugo Hens** are with KUL Laboratory of Building Physics, Leuven, Belgium, and **Anne Silberstein** and **Jean Boulant** are with CRIR Isover Saint-Gobain, Rantigny, France.

nonwoven polypropylene membrane, $d$ = 0.45 mm, $\delta$ = $1.7 \cdot 10^{-12}$ s; the membrane is also assembled in two parts with a horizontal overlap.

### Field 3

- The same as Field 1, except that a vapor-tight underroof is placed in the wooden frame: a bituminous impregnated membrane of polypropylene fibers, $d$ = 0.55 mm, $\delta$ = $6.2 \cdot 10^{-15}$ s; the sheet is assembled in one part without overlaps; field 3 functions as a reference for the measurements, a roof with a vaportight underroof.

### Measuring Points, per Field

- Temperatures on the surface of each layer were measured at 5 heights on both sides of the insulation (at 30, 69, 106, 143, and 180 cm from the bottom edge, along the slope) and at three heights on the inner surface of the gypsum board, the outer surface of the underroofs, and both sides of the tiles (at 30, 106 and 180 cm).
- Air pressures on the inner surface of the gypsum board, in between the gypsum board and the insulation, in between the insulation and the underroof, in the cavity under the tiles and on the outer surface of the tiles, measured at 30, 106, and 180 cm.
- Heat fluxes on both sides of the insulation, measured at two heights, 30 and 180 cm.

## Measuring Scheme

As shown in Figure 2, the test roofs are mounted between a hot box and cold box that simulate interior and exterior conditions. The experiment is developed in three stages, during which convection becomes more and more important. An air pressure difference can be generated over the test roofs by means of a fan group connected to the hot box. The test was started on August 1, and the last measurement took place December 17, 1991. Temperatures, heat flows, and relative humidities were continuously recorded; the output consists of the weekly averaged values and standard deviations. Air pressures and airflow rate were measured at the end of each week. Moisture migration through the construction was mapped weekly by weighing the parts of the three roof sections. To judge the amount of water that had run off the underroofs, a small gutter was installed at the bottom of each roof. (For reasons of readability, the "partial pressure of water vapor" is referred to as "vapor pressure.")

### Stage 1: Diffusion

- Duration: nine weeks.
- A constant temperature and vapor pressure difference is maintained as well as possible between hot and cold box; average conditions: $\Delta\theta$ = 20.5 °C; $\Delta p$ = 750 Pa.

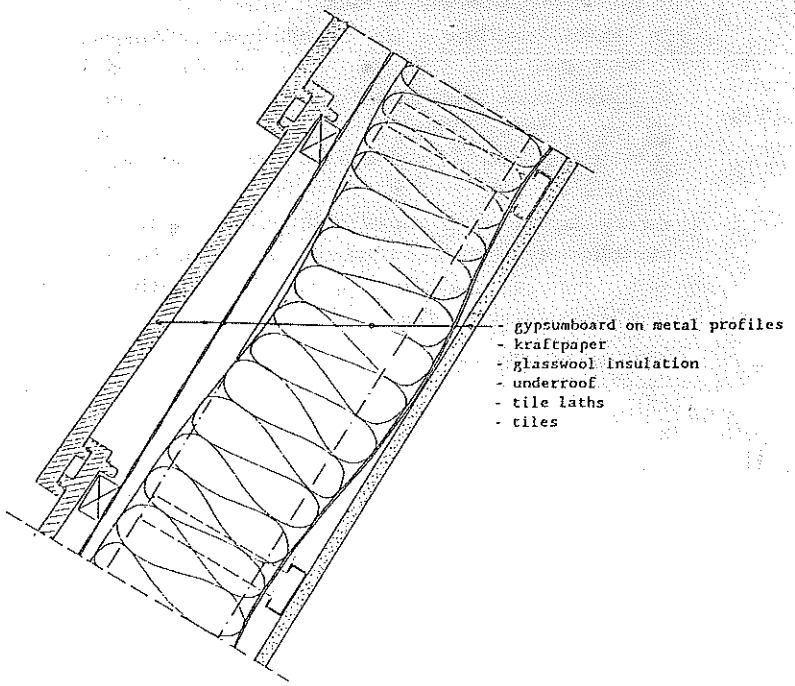


*Figure 1 Roof section.*

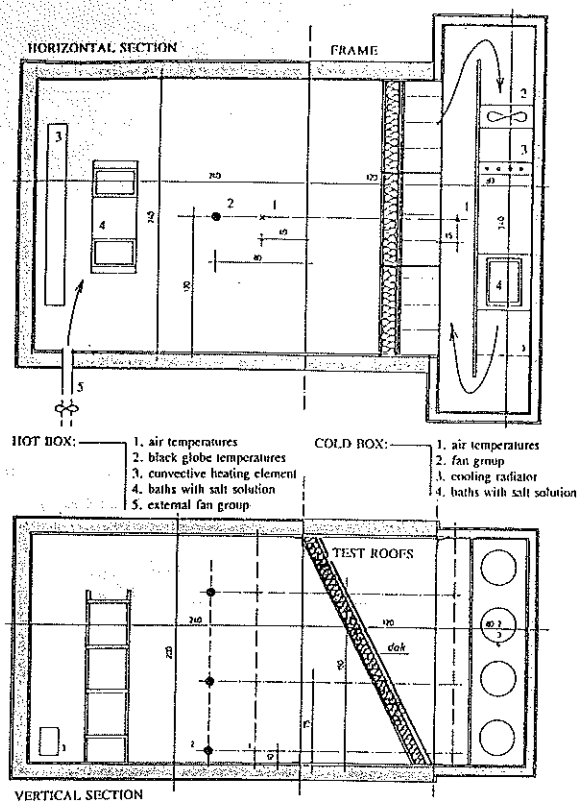


*Figure 2 Hot and cold box.*

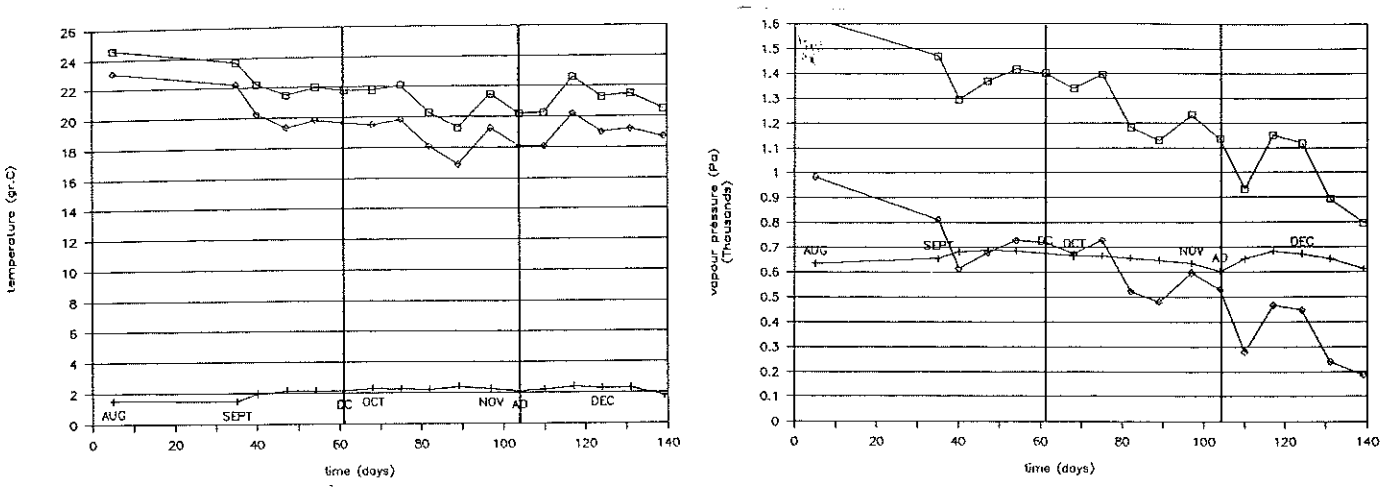


*Figure 3 Temperature (left) and vapor pressure (right) vs. time (□ hot box, + cold box, ◇ difference).*

**Stage 2: Diffusion-Convection, Airtight Construction**

- Duration: six weeks.
- A constant temperature, vapor pressure, and air pressure difference is maintained as well as possible between hot and cold box: $\Delta\theta$ = 18.5 °C; $\Delta p$ = 590 Pa; $\Delta p_a$ = 10.5 Pa.

**Stage 3: Diffusion-Convection, Air-Open Construction**

- Duration: five weeks.
- A constant temperature, vapor pressure, and air pressure difference is maintained as well as possible between hot and cold box: $\Delta\theta$ = 19.0 °C; $\Delta p$ = 325 Pa; $\Delta p_a$ = 4.5 Pa.
- The roofs are made air-open by sawing two horizontal grooves (width = 0.3 cm, length = 26.0 cm) in the gypsum board at 52.0 cm (along the slope) from the bottom and the top, simulating the placing of plaster board with open joints.

## BOUNDARY CONDITIONS

### Temperature, Vapor Pressure, Relative Humidity

It appeared to be impossible to maintain the temperature and vapor pressure difference between the hot and cold box at a constant level during the total measuring period because the laboratory where the tests were done was not conditioned and humidification in the boxes was done by free evaporation. From the moment that the fan group is connected to the hot box, the temperatures and vapor pressures become less stable (Figure 3). With increasing airflow rate (stage 3), the relative humidity falls in the hot box while it rises in the cold box; by convection, more moisture is transported through the construction. The first effect is also due to the very dry conditions in the laboratory; as a consequence, the vapor pressure difference between the hot and cold box drops continuously.

### Air Pressure

When comparing heat loss and moisture migration in the three roof sections, it is important to know that air pressure differences differ from field to field and fluctuate as a function of height.

This differentiation is due to a distribution of pressures in the cold box. The fan group in the box creates an airflow from field 1 to field 3, generating wind pressures; the irregular shape of the flow section explains the large differences over the pressure field (Figure 4). Measurement of the air pressures on the outside surface of the tiles and on the inside surface of the gypsum board during stage 1 showed that even then we were not observing "pure diffusion" alone and that we have to take convection into account. Some air flows from the hot box through the roof construction of field 1 and 2 to the cold box and back to the hot box through field 3. Averaged pressure differences during stage 1, as measured at three heights, are given in the following table; the air pressure in the hot box is taken as a reference, and a positive pressure difference means resulting airflow from the cold box to the hot box.

| Place | Height (cm): | 30 | 106 | 180 |
|---|---|---|---|---|
| Field 1 | *(Pa)* | -1.4 | -2.6 | -1.2 |
| Field 2 | | -3.3 | -2.2 | -3.1 |
| Field 3 | | 0.9 | 1.0 | -0.1 |

## THERMAL PERFORMANCE

### Temperatures and Airflows

Figure 5 shows the averaged values of the measured temperature ratios per stage. These temperature profiles give an indirect picture of the complicated way air moves in and through the roofs, which is caused by the following effects.

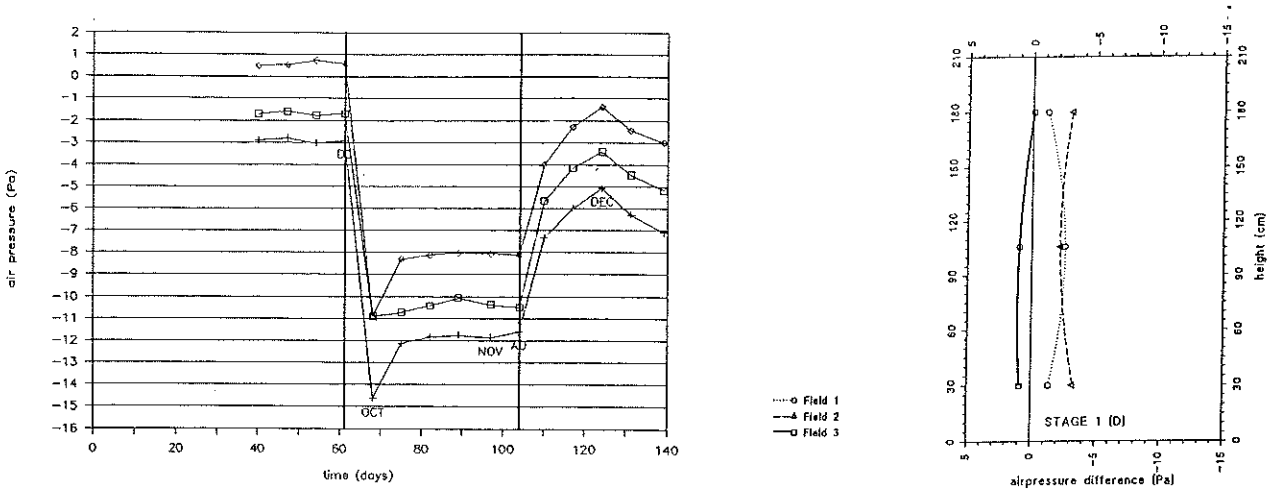


***Figure 4*** *Air pressure difference vs. time (left: □ field 1, + field 2, ◇ field 3) and vs. height (right: stage 1).*

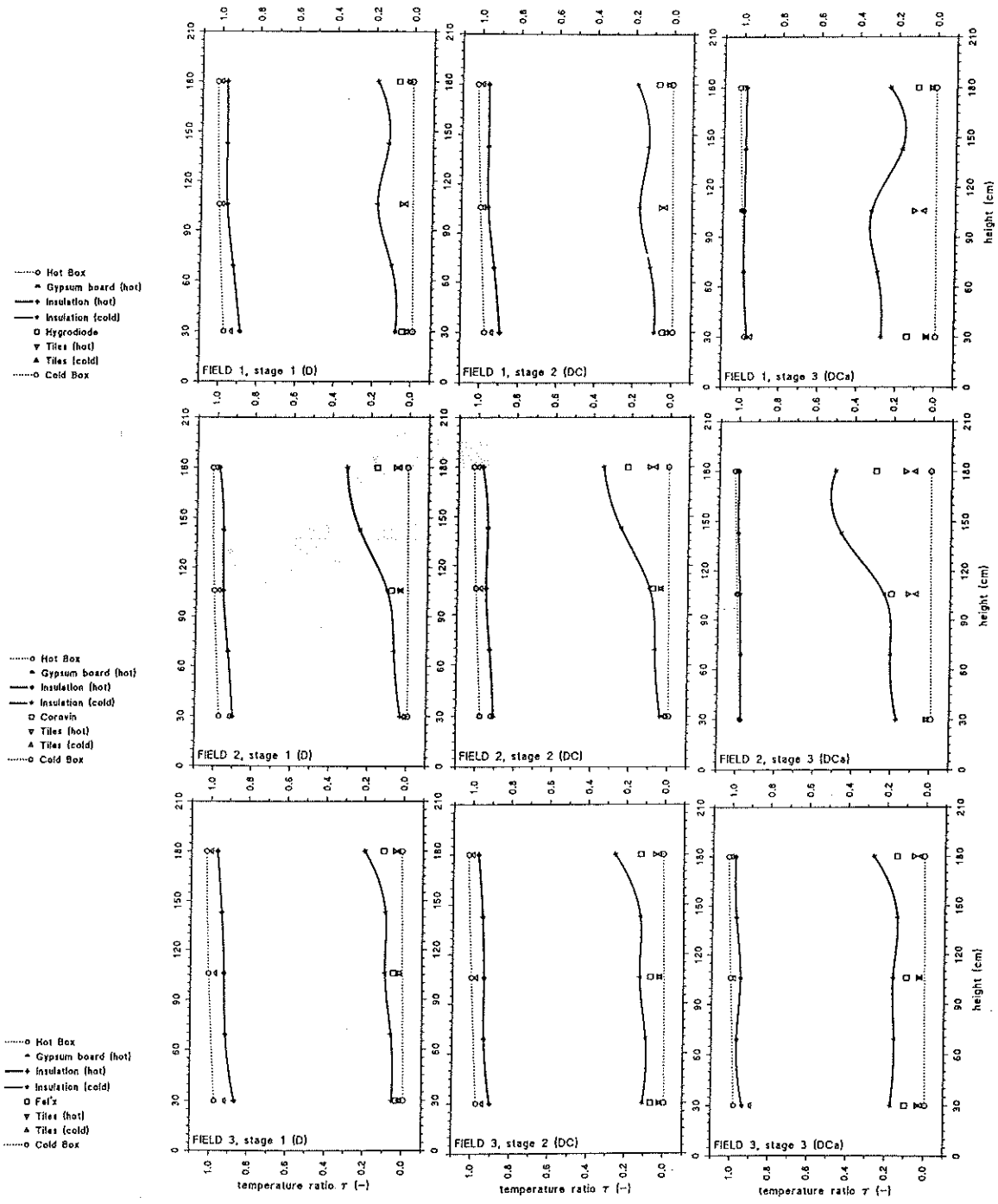


***Figure 5*** *Averaged measured temperature ratios in fields 1, 2, and 3 per stage.*

**Natural Convection** Natural convection is directly linked to air density differences induced by temperature differences and resulting in rotative stack flow in and around the insulating layer; air is warmed up at the inner side of the insulation layer, rises along the warm surface, and infiltrates through the insulation to the cold side, causing higher temperatures at the top of the outside surface of the insulation. Here the air cools down again, drops along the cold surface, and flows back to the warm side, causing locally lower temperatures.

**Forced Convection** Forced convection is linked to air pressure differences and to a lack of airtightness. Convective airflows cause the temperature change across a construction to become exponential rather than linear.

This results in small temperature gradients on the inside of the insulation layer and large gradients on the outside of the insulation in the case of a positive global airflow rate, moving from inside to outside. The opposite happens in case of a negative airflow rate (Hens 1992). The more air open a construction and the bigger the airflow through it, the stronger the influence on the temperature gradient. Forced convection also reduces the effect of stack flow, without canceling it; air velocities through the insulation layer are equalized along the height of the construction. This is also stronger in more air-open constructions.

During stage 3, the grooves made in the gypsum board result in a high air-openness of the roofs and bigger airflow rates than before. The effects are clear: the temperatures of the gypsum board and at the warm surface of the insulation become equal to those in the hot box, while the temperatures of the layers on the cold side of the insulation (underroof and/or tiles) differ greatly. The opposite is measured during stage 1 in field 3, where a negative airflow exists; here the temperatures of the layers on the warm side of the insulation diverge more in comparison with stage 2. Because field 3 is the most airtight (underroof without overlaps), the effect is less pronounced.

**Geometry** Air density and air pressure differences do not result in homogeneous airflow fields. Airflows search for the easiest way to move into and out of a construction. Therefore, convective (both thermic as well as hygric) effects can be local and very concentrated at the most air-open parts of a construction or layer (leaks, grooves, overlaps). In the temperature profiles, these parts are easily identified.

For example, in field 1, the local increase of temperature at the center of the outside insulation surface is caused by the overlap in the underroof (at 100 cm) to which the airflows are directed. This also explains the increase of temperature at the top and bottom of the same plane; here the joints "underroof - measuring frame" are situated, introducing a horizontal leak (at 0 and 210 cm).

**Cold Box Air Infiltration Due to Lack of Windtightness** As already stated, the "wind" in the cold box creates a complicated pressure field, not only causing a distribution of air pressure differences over the separate fields, but also causing infiltrating airflows from the cold box to the insulation layer and back to the cold box. The temperature drop at the center of the layers on the cold side of the insulation in field 2 might be explained by such a local cold box flow; pressure measurements revealed a higher pressure in the middle of the tile deck.

To reveal this cold air infiltration in an objective way, a tracer gas test was done during stage 2. During the test, $SF_6$ was released in the hot box to maintain a constant concentration of $\pm$ 20 ppm. The change of tracer gas concentration with time was scanned in field 1 on both sides of the gypsum board, in between the insulation and underroof, and on both sides of the tiles: $h$ = 106 cm (Figure 6).

The measurements reveal an intensive mixing of air around the tiles; no significant difference is measured between the concentration on the outside surface of the tiles and in the cavity between the tiles and underroof. Further, the airspace in between the insulation and gypsum board reacts immediately on concentration changes in the hot box, which shows the quick dynamics of airflows.

Figure 6 clearly indicates the reality of cold air infiltrating into the construction through joints and overlaps; although no channels are installed to vent the underroof, the airspace in between the underroof and insulation contains 50% cold box air, while the space between the gypsum board and insulation still contains 25% cold box air (see the stationary period during the test).

From an energy point of view, this phenomenon is distinctly negative; from a hygric point of view, it is positive (see hygric performance).

## Heat Flows and Local Air Velocities

**Heat Flows** Heat flow sensors measure a signal proportional to the local temperature gradient. By calibrating them, the local conductive heat flux can be derived. The one-dimensional conduction law states:

$$q_{cond} = -\lambda \cdot \frac{\partial T}{\partial x} \quad (1)$$

where

$q_{cond}$ = conductive heat flux (W/m$^2$),
$\lambda$ = thermal conductivity (W/(m·K)),
$\partial T/\partial x$ = temperature gradient in $x$-direction (K/m).

When air flows through a construction (no matter whether it is induced by temperature or by pressure differences), the temperature change across the section goes from a linear to an exponential one, making temperature gradients—and thus measured heat fluxes—change with position (Hens 1992). This results in small gradients, where the air flows into an insulation layer, and large gradients, where the air flows out. So also here, heat flow profiles give an indirect picture of the airflow field.

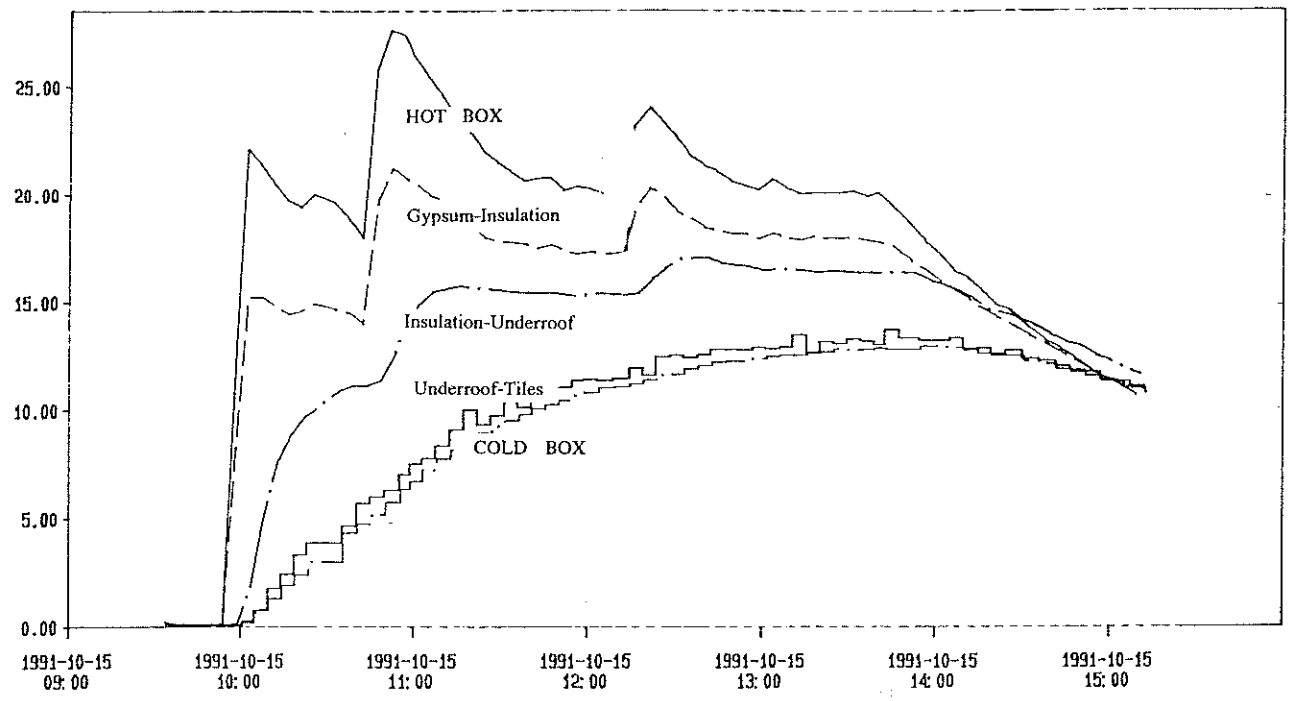


*Figure 6 Tracer concentration in the layers of field 1 vs. time during constant concentration in hot box.*

**Calculating Local Air Velocities from Measured Heat Flows (One-Dimensional)** When taking convection into account (airflow from inside to outside), Equation 1 changes into

$$q = -\lambda \cdot \frac{\partial \theta}{\partial x} - g_a \cdot c_a \cdot \theta \qquad (2)$$

where

$g_a$ = airflow density (kg/(m$^2$·s)),
$c_a$ = specific heat capacity of air (J/(kg·K)),
$\theta$ = temperature (°C).

Assuming stationary conditions, we can write the conservation law for heat transfer as

$$\frac{\partial q}{\partial x} = 0 \; . \qquad (3)$$

Taking $\theta = \theta_{se}$ = temperature on the cold side of the insulation, for $x = 0$, and $\theta = \theta_{si}$ = temperature on the warm side of the insulation, for $x = d$, the temperature curve over an insulation layer can be obtained:

$$\theta(x) = \frac{\theta_{si} \cdot (1 - e^{-\frac{Pe.x}{d}}) - \theta_{se} \cdot (e^{-Pe} - e^{-\frac{Pe.x}{d}})}{1 - e^{-Pe}} \qquad (4)$$

where

$$Pe = \frac{g_a \cdot c_a}{\frac{\lambda}{d}}, \qquad (5)$$

Pe = the Peclet-number (-).

The total heat flow follows from Equation 2:

$$q = -\frac{g_a \cdot c_a \cdot (\theta_{si} - \theta_{se} \cdot e^{-Pe})}{1 - e^{-Pe}} \; . \qquad (6)$$

By calculating the derivative of the temperature, the local conductive heat flow curve is known:

$$q_{cond}(x) = -\lambda \cdot \nabla\theta = -\frac{g_a \cdot c_a \cdot e^{-\frac{Pe.x}{d}}}{1 - e^{-Pe}} \cdot (\theta_{si} - \theta_{se}) \; . \qquad (7)$$

Now, by introducing the material properties of the insulation layer and the measured temperatures on both surfaces in Equation 7 and by plotting the relationship $q_{cond}(x)$ - $q_{measured}$ as a function of $g_a$ for the different measuring points (both $x = 0$ as $x = d$), we can find the local air velocities on both surfaces of the insulation layer for the different heights. The intersection between the curves and the $x$-axis marks the air velocity at which the theoretical conductive heat flow equals the measured one.

The values found are the velocity components perpendicular to the roof slope. With this calculation, the implicit assumption is made that the air velocity at a given height through the insulation is a constant. This can only be judged as correct if the velocity values found on both sides of the insulation are the same per height.

**Local Air Velocities** In Figure 7, the observed minimum and maximum air velocities through the insulation layer are plotted as a function of height. Since the inside surface of the insulation is covered with a kraftpaper layer, we observe three- rather than two-dimensional airflows. This explains the systematic differences between the local air velocities on the warm and cold sides of the insulation.

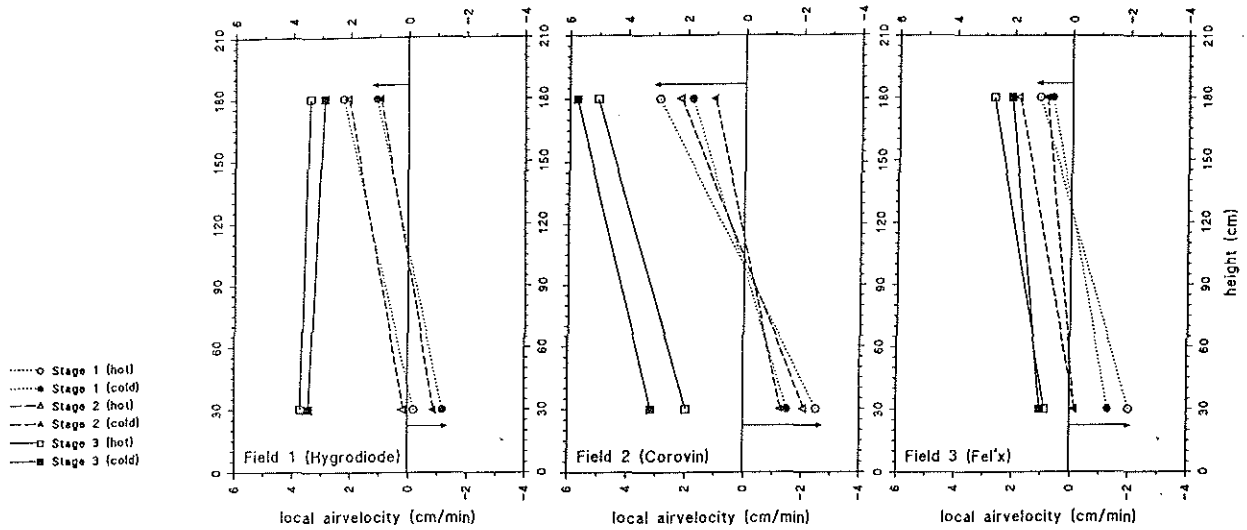


*Figure 7 Local air velocities per field, averaged per stage, as a function of height.*

However, they give a good summary of the phenomena outlined higher.

As a comparison, the measured airflow rates are recalculated to average velocities through the roofs: stage 2, 2.0 cm/min $\leq v_{avg} \leq$ 2.1 cm/min; stage 3, 3.9 cm/min $\leq v_{avg} \leq$ 6.0 cm/min.

## Consequences for Energy Efficiency

| * *U*-value | *d* (m) | λ (W/m·K) | $R_{eq}$ (m²·K/W) |
|---|---|---|---|
| Gypsum board | 0.012 | | 0.12 |
| Airspace | 0.01 | | 0.15 |
| Insulation | 0.14 | 0.041 | 3.41 |
| Airspace | 0.02 | | 0.17 |
| Tiles | | | 0.06 |

Assuming $h_i$ = 8 W/(m²·K) and $h_e$ = 23 W/(m²·K), $U$ = 0.24 W/(m²·K)

**Estimated Increase of Heat Losses Due to Airflows** If surface temperatures on both sides of the insulation and local air velocities as a function of height are known, the total heat flow through the insulation can be estimated with Equation 6. The variation of velocity with height is assumed to be linear. Calculating the total heat flow at five heights, using both values of velocity found (calculated on cold and warm side of the insulation), results in an estimation of the increase of *U*-value expressed by the factor

$$\gamma = (U_{actual} - U_{theoretical}) / U_{theoretical} .$$

| | Stage 1 | Stage 2 | Stage 3 |
|---|---|---|---|
| Field 1 | 2% ≤γ≤ 64% | 5% ≤γ≤ 69% | 223% ≤γ≤ 255% |
| Field 2 | 19% ≤γ≤ 35% | -2% ≤γ≤ 17% | 255% ≤γ≤ 335% |
| Field 3 | -12% ≤γ≤ -10% | 20% ≤γ≤ 50% | 98% ≤γ≤ 115% |

The increase in heat loss during stages 1 and 2 is merely due to rotative stack flow and a lack of windtightness: $\gamma_{avg}$ = 25%; because of the airtightness of the gypsum board, pressure differences between the hot and cold boxes do not result in alarming energy losses through the roofs. The order of magnitude of γ corresponds to values found in the literature for constructions insulated with low-density mineral wool (Lecompte 1989). The increase of heat loss during stage 3 seems to be inadmissible. However, those high values are a consequence of the hypothesis; they give an interpretation of the heat loss through an envelope part as an independent system without looking to what happens in a room that is separated from the outside by this envelope. When air flows through a construction from inside to outside, this implies that air flows in from the outside climate through another envelope part of the building, locally resulting in heat gains (for instance, field 3, stage 1). The actual heat loss then consists of conductive and ventilative losses. From this point of view, air-open constructions are very critical in relation to energy loss, since small air pressure differences generate uncontrolled ventilation rates and deteriorate the thermal qualities of the building.

## HYGRIC PERFORMANCE

### Development (Figures 8 and 9)

**Field 1** The hygrodiode membrane, used here as an underroof, was originally conceived as a vapor retarder to be adapted in flat-roof constructions: sufficiently impermeable for vapor but permeable to liquid water (Korsgaard 1985). The membrane consists of a synthetic fabric with good capillary suction properties, sandwiched between stripes of diffusion-tight plastic film staggered with an overlap. It is because of its capillarity that the hygrodiode was tested for its behavior as an underroof.

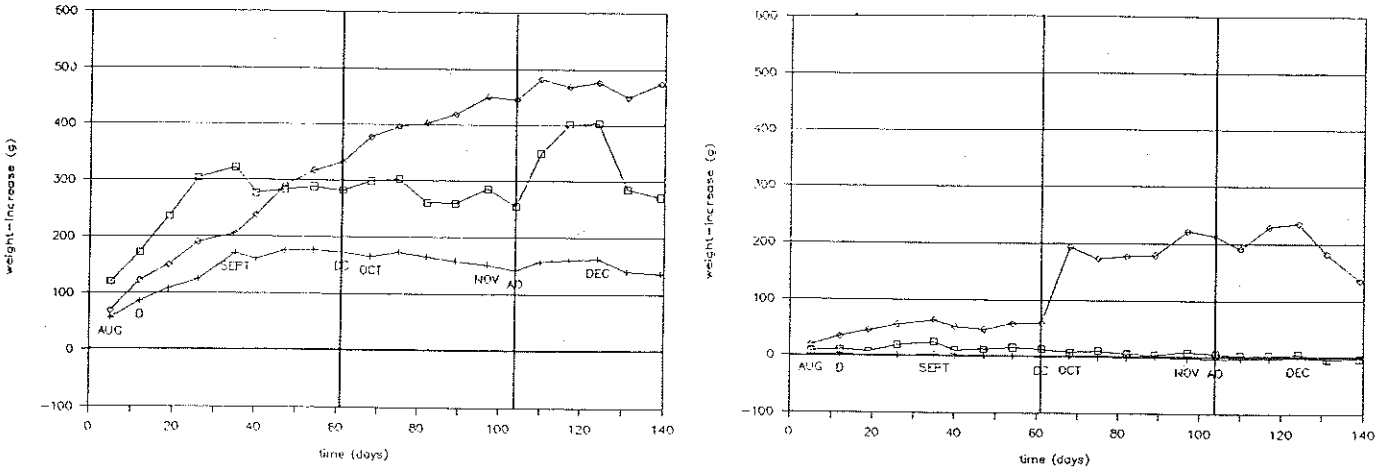


*Figure 8* *Weight increase, underroofs (left) and insulation (right) vs. time (□ field 1, + field 2, ◇ field 3).*

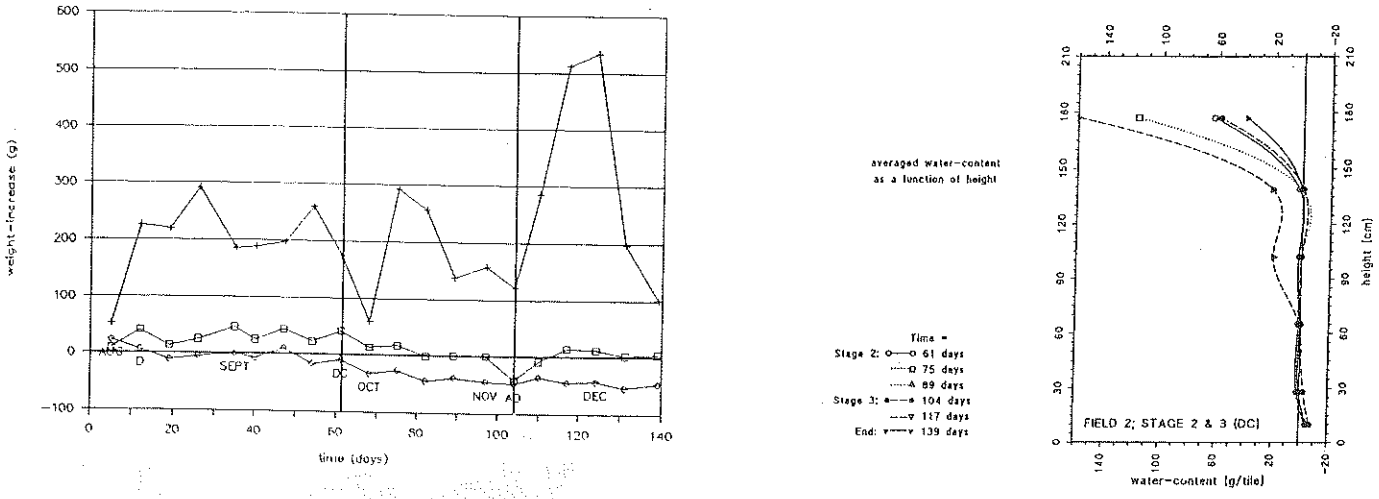


*Figure 9* *Weight increase, tiles vs. time (left: □ field 1, + field 2, ◇ field 3) and vs. height (right: field 2).*

From the first test week, condensation was clearly present against the underroof, allthough not uniformly over the whole surface. During stages 1 and 2 (airtight construction), only the upper half of the hygrodiode was wetted. Droplets of condensate stick at the plastic stripes, while the synthetic fabric becomes saturated. Though visible condensation never disappears, the weight increase stops after a month and reaches a plateau at 275 g. It is only during stage 3, when grooves are sawn in the gypsum board, that the weight increase rises again until 400 g is reached. Now condensation is visible from top to bottom. At the end of the test, the vapor pressure difference between the hot and cold boxes has reached such a low limit that the bottom part of the hygrodiode and the zone around the overlap are drying again. Except for some tiny droplets during stage 3, no water runoff was noticed in the gutter. Tiles and insulation do not show significant differences of weight increase.

**Field 2** Since the diffusion resistance of the spunbonded corovin sheet is very low, the critical condensation plane is switched from the underroof to the tile deck. Except for some small drops sticking at the upper corner of the underroof during stage 3, the underroof stays dry during the measuring period. The measured increase of weight is only due to the hygroscopical wetting of the wooden underroof frame.

During the first two stages, the weight increase of the tiles fluctuates constantly around 200 g and is completely situated at the upper tile row (w = ± 60 g/tile = ± 37 kg/m$^3$); though no condensation drops appear, the tiles become distinctly wet. Little mold spots also start growing around the joints of the upper tile row, until at the end of stage 2, the inner tile surfaces are completely moldy. During stage 3, more mold spots start growing on the tiles of the second and third row. The weight increase rises to another plateau around 520 g. At that moment, the tiles of the upper row contain ± 160 g water per tile or w = ± 100 kg/m$^3$ (Figure 9). This water content is half of the capillary water content. No water drops are noticed.

**Field 3** The bituminous underroof membrane, with a high diffusion resistance, is executed without overlap. During all the stages, interstitial condensation is clearly

present, with a pronounced peak against the upper half of the sheet. The middle rafter of the field is marked as a dry(er) zone on the underroof. From the moment that wet hot-box air is blown through the test roofs, water starts to drip off the underroof in an amount of ± ¼L/week. The underroof also absorbs water from the condensation plane, and the weight increases progressively.

The weight of the insulation follows the course of the condensation against the sheet. Water dripping off can be seen as drops spread out over the insulation surface, wetting the upper surface layer. Since water is not absorbed by the glasswool, the weight reaches a platform at 200 g.

## Interpretation

**One-Dimensional Diffusion Calculation (Glaser 1959)** Because of the continuous decrease of the vapor pressure difference during the three stages, the interpretation of the results becomes difficult. Changes in hygric behavior can not be judged in an independent way since the causes are interrelated. By executing a condensation calculation using the measured vapor pressures and the averaged measured temperatures at the condensation planes as boundary conditions, the effects of airflows on the hygric behavior of the roofs can be judged independently from effects caused by vapor pressure changes.

First, the influence of diffusion leaks (joints, overlaps, perforations) on the diffusion thickness $\mu d$ (m) of kraftpaper and underroofs is calculated with a two-dimensional stationary model.

| Results | $\mu d$ (m) | $\mu d_{eq}$ (m) | $\mu d_{calc}$ (m) |
|---|---|---|---|
| Hygrodiode | 1.79 | $0.78 \leq \mu d \leq 1.11$ | 0.80 |
| Corovin | 0.047 | $0.045 \leq \mu d \leq 0.06$ | 0.045 |
| Fel'x | 15.85 | $1.26 \leq \mu d \leq 2.41$ | 1.70 |
| Paper | 4.95 | $0.50 \leq \mu d \leq 0.56$ | 0.53 |
| Gypsum board | 0.10 | | 0.10 (0.01) |
| Tiles | | | 0.12 |

The weight increase of the underroofs of fields 1 and 3 (hygrodiode and fel'x) and the tiles in field 2 as calculated is shown in Figure 10.

A linear regression gives the following condensation flow rates against the underroofs per stage (since for August no measured boundary conditions are available, the given value for stage 1 is the averaged moisture flow during September). The effect of the lower vapor pressure difference is clear:

| | St 1 | | St 2 | | St 3 | |
|---|---|---|---|---|---|---|
| (G/Day) | Avg | Std | Avg | Std | Avg | Std |
| Field 1 | 15.5 | 0.5 | 9.6 | 0.7 | -0.5 (First 2 weeks) | 2.8 |
| Field 3 | 18.2 | 0.3 | 11.2 | 0.6 | 3.4 | 1.1 |

The tiles in field 2 hardly become 250 g heavier; they start drying from stage 2.

**Comparison (Figure 10)** A linear regression gives the following measured condensation flow rates per stage, including the sum of the amounts of condensation measured in the underroof, insulation, and gutter and reduced with the hygroscopic weight increase measured in the wooden underroof frame (the weight of the underroof in field 2 is taken as a reference).

| | August | | St 1 | | St 2 | | St 3 | |
|---|---|---|---|---|---|---|---|---|
| (G/Day) | Avg | Std | Avg | Std | Avg | Std | Avg | Std |
| Field 1 | 7.0 | 0.8 | -1.5 | 1.0 | -0.2 | 0.5 | 9.7 (First 2 weeks) | 1.6 |
| Field 3 | 4.5 | 0.4 | 4.7 | 0.3 | 33.1 | 2.5 | 37.6 | 3.0 |

By comparing calculated and measured condensation flow rates, condensation appears to be overrated by the diffusion calculation (two to four times higher) during stage 1; this is due to a lack of windtightness of the underroof system (see "Cold Box Air Infiltration"). During stages 2

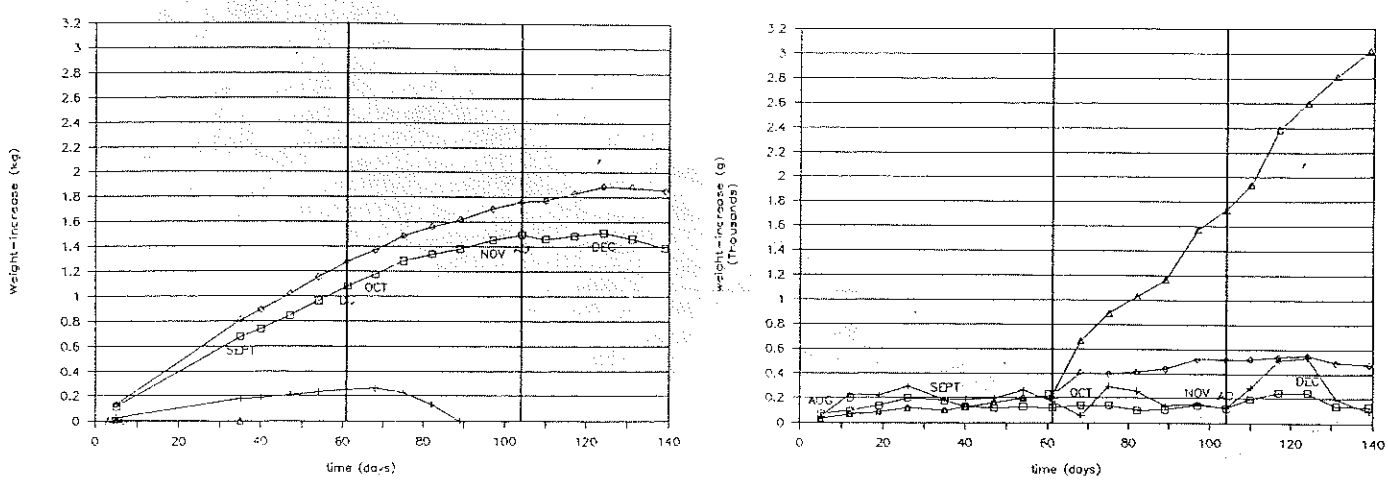


*Figure 10 Calculated (left) and measured (right) condensation: □ 1: underroof, + 2: tiles, ◇ 3: underroof, ▵ 3: runoff.*

and 3, the real condensation amounts in field 3 are much more alarming than predicted by diffusion only. The capillary underroof in field 1 (hygrodiode) behaves distinctly differently from the vaportight sheet in field 3.

### Hygric Behavior: Global Interpretation

1. Natural and forced convection in and through a construction, together with (two- or three-dimensional) changes in geometry, make moisture migration and condensation a local, nonhomogeneous phenomenon. Due to rotative stackflow, the upper parts of the condensation plane(s) are wetted first.
2. Convection from inside to outside makes the condensation behavior of a construction very sensitive to tiny changes in air-openess or in boundary conditions.

   Unlike diffusion, convection is a quick phenomenon, able to transport larger amounts of moisture through a construction, and is, therefore, more important. When a moist airflow in a construction meets a cold surface, the vapor condenses against the surface if the temperature of the surface is lower then the dew point of the air. The bigger the airflow rate, the more vapor reaches the cold surface and the greater the condensation amount becomes—at least as long as the surface temperature does not rise above the dew point of the air. Indeed, airflow also creates enthalpy flows, making the temperatures in the construction rise. Figure 11 shows this more clearly: here the condensation flow rate as a function of the air pressure difference is calculated for field 3, with a one-dimensional analytical model, taking enthalpy and latent heat flow into account. The curves are plotted for two values of the air permeance of the gypsum board, with the vapor pressure difference over the construction as a parameter. For air-open roofs, a condensation peak is predicted at rather low air pressure differences. Once the air pressure difference becomes higher than the critical difference, the condensation amount diminishes again.

   The above phenomenon makes condensation in air-open constructions very critical. A small change in air permeance, air pressure difference, or vapor pressure difference can either result in alarming condensation flow rates or in a sudden drying.
3. Also with convection, variations of the condensation flow rate stay directly dependent on variations of the vapor pressure difference (the airflow rate being a constant)
4. Capillarity of the possible condensation plane (field 1: the hygrodiode membrane) plays an important role in the hygric behavior of the roof. First, the underroof acts as a moisture buffer, causing a rise in the moisture content until an equilibrium is reached between condensation on the inside and drying from the outside surface; the underroof weight reaches a constant level. Due to rotative stack flow, a moisture content gradient over the height of the underroof exists, until more humid air flows through the envelope (stage 3) and the bottom part of the membrane is wetted. As a consequence, the underroof becomes heavier again until a new wetting-drying equilibrium is reached. This property returns interstitial condensation to a harmless phenomenon.

## CONCLUSIONS

The test results show that the amount of water vapor migrating into a sloped roof by diffusion is insignificant compared to the amount that enters the construction by convection through leaks in the finishing layer. Air-open roofs with a vapor-tight underroof are very sensitive to this effect that may quickly lead to serious condensation problems. Since experience has shown how rarely a finish is installed to be airproof, preventions should be taken. A solution against possible moisture damage caused by convective vapor flow is the use of a vapor-open, hygroscopic and/or capillary underroof.

$\theta_i = 21°C$, $\theta_e = 2.5°C$, $p_e = 675$ Pa;
+ Δ ∇: airopen roof
$K_a(\text{gypsum}) = 6.3*10^{-4}*\Delta p_a^{-0.27}$ s/m;
□ ◇ x: airtight roof
$K_a(\text{gypsum}) = 3.1*10^{-5}*\Delta p_a^{-0.19}$ s/m;

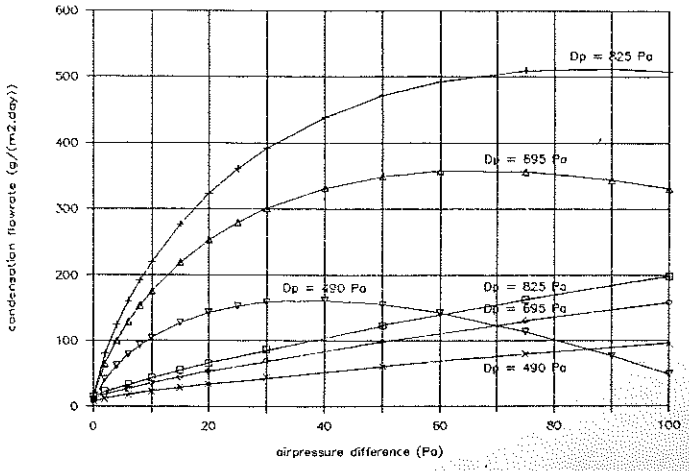


*Figure 11 Calculated condensation flow rate at the underroof of field 3 vs. air and vapor pressure difference.*

From an energy point of view, the attachment of an air barrier on the inside of the insulation, executed in such a way that perforation and rupture are avoided, is a necessity. The test results further show that rotative stack flow and infiltration of cold air reduce the thermal quality of the roof construction by 20% to 30%. To reduce this estimated energy loss, the insulation material should be installed as a sandwich in between the air barrier and underroof, without open joints or cavities.

To measure the influence of such parameters as thickness and density of the insulation layer and wind-tightness of the underroof on the energy loss through an insulated roof, further research is needed.

## ACKNOWLEDGMENTS

This research project became possible thanks to the Flemish Ministry of Regional Economy and Energy in the frame of the IEA-Annex 24 project on Heat, Air and Moisture Transfer in Insulated Envelope Parts and by grants of the industry. It was executed at the Laboratory of Building Physics, KU, Leuven, Celestijnenlaan 131, B-3001 Leuven (Heverlee), Belgium, in cooperation with ISOVER NV Saint Gobain, Rantigny, France.

## REFERENCES

De Groeve, A., and D. Van Lokeren. 1991. *Hellende daken met isolatie in het dakschild: inwendige kondensatie ten gevolge van diffusie en convectie, eindverhandeling* (Sloped roofs with side-insulation: interstitial condensation caused by diffusion and convection). Graduation dissertation, KIH Oost-Vlaanderen, Gent, 103 pp.

Glaser, H. 1959. *Grafisches Verfahren zur Untersuchung von Diffusionsvorgänge.* Kältetechnik, n°10.

Hens, H. 1992. *Bouwfysica 1: warmte en massatransport* (Building Physics 1: heat and mass transfer). Acco Leuven, 218 pp.

Hens, H., W. Uytterhoeven, F. Vaes, and L. Neyrinckx. 1983. *Globale vochtgedrag van hellende daken* (Overall moisture behaviour of sloped roofs). Rapport onderzoek WTCB- KU Leuven - IWONL, conventie 3687, 82 pp.

Hens, H., J. Lecompte, G. Mulier, and P. Staelens. 1986. *Globale vochtgedrag van hellende daken* (Overall moisture behaviour of sloped roofs). Rapport onderzoek WTCB - KU Leuven - IWONL, conventie 4213, 94 pp.

Hens, H. 1992. *Pitched roofs: heat-air-moisture transport in tiled and slated roofs with the thermal insulation at rafter level.* IEA-Annex 24 Internal Report T4-B-1992/01, Labo Bouwfysica KU Leuven, 98 pp.

IEA-Annex 14. 1991. Condensation and energy, Volume 1, *Sourcebook.* Acco Leuven.

IEA-Annex 14. 1991. Condensation and energy, Volume 3, *Catalogue of Material Properties.* Acco Leuven.

Janssens, A. 1991. *The influence of airflows on the hygro-thermal behaviour of sloped insulated roofs: A case study.* IEA-Annex 24 Internal Report T4-B-1991/2, Labo Bouwfysica KU Leuven, 16 pp.

Korsgaard, V. 1985. Hygro diode membrane: A new vapour barrier. *Thermal performance of the exterior envelopes of buildings.* Atlanta: American Society of Heating, Refrigerating and Air-Conditioning Engineers, Inc.

Lecompte, J. 1989. *De invloed van natuurlijke convectie op de thermische kwaliteit van geïsoleerde spouwconstructies, doctoraal proefschrift* (The influence of the stack effect on the thermal quality of insulated cavity constructions, doctoral dissertation). KU Leuven, 206 pp.